

PREPARATION AND CHARACTERIZATION OF LANTHANUM OXIDE DOPED BARIUM STRONTIUM TITANATE PARAELECTRIC GLASS CERAMICS

Swonal Sitam Das



Department of Ceramic Engineering
National Institute of Technology, Rourkela
Rourkela - 769008, India

PREPARATION AND CHARACTERIZATION OF LANTHANUM OXIDE DOPED BARIUM STRONTIUM TITANATE PARAELECTRIC GLASS CERAMICS

Dissertation submitted in

June 2015

To the department of

Ceramic Engineering

Of

National Institute of Technology, Rourkela

In partial fulfilment of the requirements

for the degree of

Bachelor of Technology

By

Swonsl Sitam Das

(Roll 111CR0585)

Under the supervision of

Prof. Partha Saha



Department of Ceramic Engineering
National Institute of Technology, Rourkela
Rourkela - 769008, India

26th June 3015

CERTIFICATE

This is to certify that the work in the thesis entitled as **“Preparation and Characterization of Lanthanum Oxide doped Barium Strontium Titanate Paraelectric Glass Ceramics”** by Swonal Sitam Das, with roll number 111CR0585, is a record of an original experimental work carried out by him under my supervision and guidance in partial fulfilment of the requirements for the award of the degree of Bachelor of Technology in Ceramic Engineering.



26/06/15

Dr. Partha Saha
Assistant Professor
Department of Ceramic Engineering
National Institute of Technology, Rourkela

ACKNOWLEDGEMENT

I would like to express my sincere and profound gratitude to the faculty advisor Dr. Partha Saha, Assistant Professor, National Institute of Technology, Rourkela for his inspiring guidance, sharing his experience and knowledge and exemplary perseverance and hospitality. This work would have been a difficult task to complete without profiting from his expertise, encouragement, valuable time and constructive criticisms. I would like to admit my deep sense of gratitude to Prof. Swadesh Kumar Pratihara, Head of the Department for his constructive suggestions and valuable time throughout the work. I would like to convey my sincere gratitude to all the faculty members for their throughout support during four years of my engineering life. I would also like express my sincere gratitude to Prof. Ranabharata Mazumder for extending the facilities of dielectric measurements for completing the project in a timely manner.

I would express my gratitude to Mr. A. Kumar, Mr. P. K. Mohanty for their encouragement and never ending support during laboratory work.

I would also like to convey my thanks to my batch mates Abhijit, Chinmay, Manali, Bijay and Abhinash for their support, help and cheerful company during the project work.

Finally, I would like to like to express my heart-felt gratitude to my father Mr. Swadesh Kumar Das and my sister Ms. Swati Sanita Das for being by my side during difficulties. Their loving support has been and shall always will be my most precious possession on earth.

CONTENTS

LIST OF TABLES	1
LIST OF FIGURES	2
ABSTRACT.....	4
1 INTRODUCTION	5
2 LITERATURE REVIEW AND OBJECTIVES OF PRESENT WORK	7
3 EXPERIMENTAL PROCEDURE.....	11
GLASS FORMATION AND CERAMIZATION.....	11
DIFFERENTIAL SCANNING CALORIMETERY (DSC) STUDY.....	13
DENSITY MEASUREMENT	14
PHASE ANALYSIS USING X-RAY DIFFRACTION.....	14
FOURIER TRANSFORM INFRARED SPECTROSCOPY (FTIR) STUDY...	14
FIELD EMISSION SCANNING ELECTRON MICROSCOPE STUDY,..	15
DIELECTRIC MEASUREMENT	15
4 RESULTS AND DISCUSSION.....	16
PHASE ANALYSIS OF GLASS SAMPLES.....	16
FTIR SPECTRA OF GLASS SAMPLES.....	17
DSC STUDY OF GLASS SAMPLES.....	20
DENSITY MEASUREMENT.....	24
PHASE ANALYSIS OF GLASS CERAMIC SAMPLES.....	26
MICROSTURUTAL ANALYSIS OF GLASS CERAMIC SAMPLES.....	29
DIELECTRIC ANALYSIS.....	33
5 CONCLUSION.....	38
6 REFERENCES	39

LIST OF TABLES

Table No.	Table	Page No.
Table 2.1	Role of different constituents in the present study	10
Table 3.1	Raw material used for the preparation of glass samples	13
Table 4.1	List of FTIR peaks observed for SBT base glass	18
Table 4.2	List of FTIR peaks observed for SBT base glass	19
Table 4.3	Density measurement of the glass samples before crystallization	25
Table 4.4	Density measurement of the glass ceramic samples after crystallization	25

LIST OF FIGURES

Figure no.	Figure	Page No.
Figure 2.1:	Schematic diagram of a cubic perovskite structure (a) a three dimensional unit showing $[\text{TiO}_6]$ octahedral coordination (b) A^{2+} ions in the twelve fold coordination inside the ABO_3 unit.	8
Figure 4.1	XRD pattern of $[(\text{Ba}_{0.3}, \text{Sr}_{0.7}).\text{O.TiO}_2]-[2\text{SiO}_2-\text{B}_2\text{O}_3]-[\text{K}_2\text{O}]$ glass quenched on a preheated graphite plate	16
Figure 4.2	XRD pattern of $[(\text{Ba}_{0.3}\text{Sr}_{0.7}).\text{O.TiO}_2]-[2\text{SiO}_2-\text{B}_2\text{O}_3]-[\text{K}_2\text{O}]$ glass quenched at room temperature	17
Figure 4.3	XRD pattern of $[(\text{Ba}_{0.3}\text{Sr}_{0.7}).\text{O.TiO}_2]-[2\text{SiO}_2-\text{B}_2\text{O}_3]-[\text{K}_2\text{O}]-0.1\text{mol \%}[\text{La}_2\text{O}_3]$ glass quenched at room temperature	17
Figure 4.4	FTIR spectra of (a) SBT base glass and (b) 0.1 mol % La_2O_3 doped SBT glass	20
Figure 4.5	DSC scan from room temperature to 800 °C of pre-heated plate quench base glass sample	23
Figure 4.6	DSC study of from room temperature to 700 °C of air quenched base glass sample	23
Figure 4.7	DSC study from room temperature to 800 °C of pure strontium base glass sample	24
Figure 4.8	DSC study from room temperature to 700 °C of 0.1 mol % La_2O_3 doped glass sample	24
Figure 4.9	XRD pattern of $[(\text{Ba}_{0.3}, \text{Sr}_{0.7}).\text{O.TiO}_2]-[2\text{SiO}_2-\text{B}_2\text{O}_3]-[\text{K}_2\text{O}]$ glass ceramic sample crystallized at 780°C for 3h in air	28
Figure 4.10	XRD pattern of $[(\text{Ba}_{0.3}, \text{Sr}_{0.7}).\text{O.TiO}_2]-[2\text{SiO}_2-\text{B}_2\text{O}_3]-[\text{K}_2\text{O}]$ glass ceramic sample crystallized at 780°C for 3h in air	28
Figure 4.11	XRD pattern of $[(\text{Ba}_{0.3}, \text{Sr}_{0.7}).\text{O.TiO}_2]-[2\text{SiO}_2-\text{B}_2\text{O}_3]-[\text{K}_2\text{O}]-0.1\text{mol}\%[\text{La}_2\text{O}_3]$ glass ceramic crystallized at 750°C for 3h in air	29
Figure 4.12	SEM image of SBT base glass ceramics	30

Figure 4.13	EDS analysis of flower like crystal found in the microstructure	31
Figure 4.14	EDS analysis of needle-shape crystal found in the microstructure	31
Figure 4.15	Elemental X-ray mapping showing the distributiun of elements from SBT base glass ceramic	31
Figure 4.16	SEM image of 0.1mol % La_2O_3 doped glass	32
Figure 4.17	EDS analysis on the blocky irregular shaped interconnected crystals observed in the 0.1 mol % La_2O_3 doped glass ceramic sample	32
Figure 4.18	Elemental X-ray mapping showing the distributiun of elements from 0.1 mol % doped SBT glass ceramic	32
Figure 4.19	Dielectric measurement of SBT base glass ceramics at room temperature	35
Figure 4.20	Dielectric measurement of doped glass ceramics at room temperature	35
Figure 4.21	(a) Dielectric constant and (b) loss of SBT base glass ceramics with temperature	36
Figure 4.22	(a) Dielectric constant and (b) loss of 0.1mol % La_2O_3 doped SBT base glass ceramics with temperature	37

ABSTRACT

(Ba_{0.3}Sr_{0.7})TiO₃-2SiO₂-B₂O₃-K₂O based borosilicate glass with and without 0.1 mol % La₂O₃ was successfully developed by melt-quench method. XRD and FTIR spectra of the glass sample confirms the formation of amorphous structure and presence of stretching and deformation vibrations of B-O-Si linkage and Si-O-Si bridges, respectively. Differential scanning calorimetry (DSC) of glass samples reveals that addition of 0.1 mol % La₂O₃ elevates the onset of crystallization temperature from ~600°C to ~670°C. Controlled crystallization of the glasses ~750-780°C for 3h leads to the formation of desired perovskite SrBaTiO₃ glass-ceramics. SEM-EDS analysis of the undoped glass-ceramic sample shows the formation of micron sized flower-like and needle shaped crystals. However, addition of 0.1 mol % La₂O₃ modify the crystal structure to blocky precipitates. Results from dielectric measurements suggest that space charge polarization mechanism is likely responsible for the large observed dielectric constant (~700) of the 0.1 mol % La₂O₃ doped glass ceramics sample at low frequencies.

KEYWORDS: Glass, Glass Ceramics, Perovskite, Paraelectric, Dielectric measurements

1. INTRODUCTION

Since the ancient days, glass is known as one of the key member in the field of ceramics. The usage and application of glass has been developed day by day for decorative purposes. However, glass has not been limited as one of the decorative assets. Its usage has been transformed from window panels, crockery items to armour, machinable as well as fireproof glass. After glass products successfully developed, the field glass-ceramics came into existence for engineering applications. Glass ceramics can also be known as “vitrocerams,” and are synthesized by controlled heat treatment schedules for ceramization of certain glass compositions which includes a suitable nucleating additive within it. Tremendous developments have also taken place gradually in the field of glass ceramics [1]. Due to the extensive research in this field several developmental work resulted new glass ceramic systems which benefited humankind both in specialized engineering use and also in the commercial field.

Since 1950 glass ceramics have also been as one of the technologically viable materials. There have been several advantages for glass ceramics as it is economically feasible as well as it could also be tailored easily from the glassy network to get the desirable properties. The properties of glass-ceramics are solely dependent upon their chemical composition, microstructure and their phases. These chemicals in a bulk control several factors including glass formation, nucleation, phase transition and also workability. We could call the glass-ceramics as one of the truly engineered materials which can exhibit a wide range of microstructural properties, optical properties, dielectric properties etc. Glass ceramics gave a very extensive range of its applications that include microwave randomes, microelectronic substrates and packaging. It has also got its applications in the biomedical field also. These extensive ranges of properties of glass ceramics had further increased the potential for its applications.

Glass ceramics are known to be the polycrystalline solids which can be synthesized through controlled ceramization of the glass samples. The crystallization of glass samples can be successfully done subjecting the glass samples undergo the appropriate heat treatment schedules. This results in the nucleation and growth of the crystal phases within the glass sample.

There are several advantages of glass ceramics-

- Through glass-forming technique it can be produced in mass.
- Specific nanostructure or microstructure is possible to design for a specific application.
- Porosity is zero or negligible.
- It is possible for to combine a variety of desired properties.

However, some amount of residual glass is observed in many cases even though crystallization process is taken to completion. It could be easily distinguished from glass as glasses are amorphous and non-crystalline in nature.

Glass ceramics can be produced through different techniques or routes. One of it is it could be prepared through bulk crystallization method. In this process melted glass is casted to an appropriate shape. It is then given a regulated heat treatment schedule and is kept at that temperature for some time to nucleate and grow crystals to get the desired degree of crystallinity.

The other method is sintering and crystallization of glass powder. In this method the glass powder is sintered and due to low eutectics some of the phases forms liquid at low temperature it seals the pores and developed a complex structure. However there are some drawbacks some of the phases gets crystallized and if the surface gets crystallized then the surface is pore free but the inner parts have some pores and are not pore free.

2. LITERATURE REVIEW

Barium Strontium Titanate (BST) glass ceramics is considered to be one of the potential ferroelectric glass ceramic for having high energy density dielectric materials. Previously it was found that the dielectric constant of these samples were approximately 1000 having the dielectric breakdown strength 800kV/cm. For the overall increase of the energy density refining agents were added to the melt. The rate of nucleation and growth of the grain is also taken into consideration while measuring the dielectric parameters. Hence the crystallization kinetics of the glass ceramic particles were studied properly to understand fully the role of the required BST phase and which phase can result in the increment of the energy density of the sample. A decrease in grain size will result in more grain boundaries. The defects existed at the grain boundary accelerates the thermally activated motions of defects which leads to an increase in the activation energy (which is higher than the conventionally synthesized powder ceramics).

The ratio of $\text{Ba}^{2+}/\text{Sr}^{2+}$ also plays a very important role in the phase formation as well as measurement of the dielectric parameters also. If the glass gets rich with Sr^{2+} then the sample shows paraelectric properties. And if the glass sample is rich in Ba^{2+} then the sample shows ferroelectric properties. Hence that the $\text{Sr}^{2+}/\text{Ba}^{2+}$ ratio has an enormous influence on microstructures, energy storage properties and dielectric relaxation behaviours of BST glass ceramics. It could also be observed that La_2O_3 additive alters slightly the dielectric constant but it significantly changes the microstructure of the glass ceramics and this resulted in improving the break down strength (BDS). Addition of La_2O_3 also increases optimized energy storage density as it could be observed when addition of 1.0 wt% La_2O_3 increases the energy storage density by ~2.5 times higher than the pure BST glass ceramics. Hence it could be concluded that the dielectric properties gets improved with the addition of the refining agents and preference of glass ceramic samples will increase the activation energy [2].

PEROVSKITE STRUCTURE

The perovskites structural family includes a large family of compounds those are having their crystal structures related to the mineral perovskite for example BaTiO_3 . One of the ideal form of crystal structure is cubic. ABO_3 perovskite can be portrayed as comprising of corner sharing $[\text{BO}_6]$ octahedral with the A cation possessing the 12-fold coordination site formed in the middle of the cube of eight such octahedral. The mineral perovskite gets modified to some extent [4].

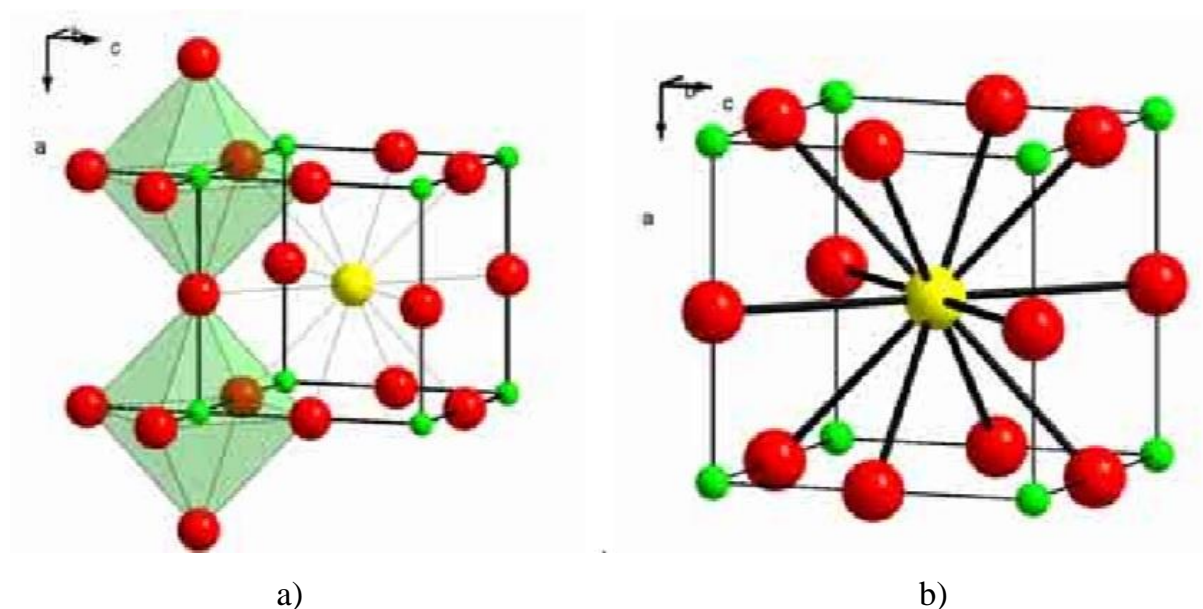


Figure 2.1 Schematic diagram of a cubic perovskite structure (a) a three dimensional unit showing $[\text{TiO}_6]$ octahedral coordination (b) A^{2+} ions in the twelve fold coordination inside the ABO_3 unit [5].

The perovskite cubic structure, e.g. found in BaTiO_3 and SrTiO_3 can be expressed as $\text{Ba}^{2+}/\text{Sr}^{2+}$ and O^{2-} ions (red) generates a cubic close packed unit where Ti^{4+} ions occupying the octahedral voids created by oxygen [6]. The perovskite structure has a three dimensional structure where $[\text{TiO}_6]$ octahedral unit share the corner and $\text{Ba}^{2+}/\text{Sr}^{2+}$ ions (green) in the twelve fold coordination between the polyhedra, according to the schematic diagram shown in **Figure 2.1** [7].

FERRO ELECTRIC GLASS CERAMICS

The theory of ferroelectric nature of glass ceramic samples are proven to be invaluable. The theory of electrical “aligning” or “poling” procedure can be identified correctly as the key to turn an inert ceramic into an electro mechanically active material have a lots of commercial uses. This can be called as one of the most unforeseen discovery, because of the prevailing opinion that ceramics can never be counted as the piezo-electric material, because the sintered and randomly oriented crystallites on the whole would, cancel out each other [3].

The oxidation state of ferroelectric materials strongly influences their performance in capacitors. Oxygen removal from the crystal lattice decreases the electrical resistivity of the material and makes it electrically conducting. There might be a chance of failure of the material by electrical breakdown when exposed to an operating temperature of 50-200°C and/or to DC electric fields exceeding of 10 volts/cm.

Oxygen loss from the perovskite lattice of ferroelectric materials usually takes place during the preparation of the material. The range of temperature for its preparation is 1100-1500°C. where oxygen's partial pressure is relatively high which results in the loss of oxygen. This loss of oxygen can be corrected by firing and slow cooling in an oxidizing atmosphere. Oxygen can have direct access into the interior of the material through the pores present in the sintered material facilitating the oxidation process. Partial crystallization of a homogeneous glass which are non-porous in nature have a considerable advantage that it provides a material of high dielectric constant and high dielectric breakdown strength, as well as other desirable electrical characteristics.

La₂O₃ DOPANT ROLE IN Sr_{1-x}Ba_xTiO₃ SYSTEM

Lanthanum oxide acts as a nucleating agent for crystallization of glass ceramics this can be observed by the crystallization of doped glass takes place at low temperature compared to the plain glass and this enhances the value of dielectric constant. These glass ceramics can be

used in making capacitors for high energy storage. This addition of La_2O_3 in barium strontium titanate glass ceramics may further increases the value of energy density. In the modification of tetragonality of barium strontium titanate phase lanthanum ions plays an important role as it gets diffused into the structure.

In La_2O_3 -doped barium titanate ceramics the La^{3+} ions replaces the Ba^{2+} cations in the A sites as La^{3+} ions are too large for the B sites where Ti^{4+} ions are present so as a result the charge is not balanced which is compensated by the cation vacancies on the A- or B-sites [8]. In addition of direct donor dopant, specifically of low donor concentration, the charge compensation mechanism and the semi-conductive characteristics were observed [9].

SEM analysis indicated that La_2O_3 additive decreases the average crystallite size. There is a significant mismatch of the peaks when the La_2O_3 concentration is 0.5 mol%. These peaks also gets separated for 1.0 mol% La_2O_3 addition obviously. With increasing La_2O_3 concentration, the crystallite impedance gets lowered, while a larger impedance can be observed for the partially crystallized glass interface. The blocking factor of the partially crystallized glass interface with the increase in the concentration of the dopant La_2O_3 . As a result the activation energy decreases only for the crystallite whereas increases for the partially crystallized glass [10].

ROLES OF DIFFERENT CONSTITUENTS

Table 2.1 Role of different phases in the present study

Phases	Role of phases
$(\text{BaSr})\text{TiO}_3$	Forms dielectric phase
$\text{SiO}_2\text{-B}_2\text{O}_3$	Glass former
K_2O	Glass intermediate
La_2O_3	Acts as dopant

OBJECTIVE

1. Prepare $(\text{Ba}_{0.3}\text{Sr}_{0.7})\text{TiO}_3$ based borosilicate and 0.1 mol % La_2O_3 doped borosilicate glass.
2. Identify the bonding modes of different constituents of the glass forming species with the help of FTIR.
3. Formation of perovskite glass ceramics by thermal treatment or control crystallization according to the DSC study.
4. Microstructural analysis and identify the different phases using X-ray diffraction analysis.
5. Determine the density of both glass and glass ceramic samples.
6. Microstructural analysis of glass ceramic samples through SEM/EDS and X-ray elemental mapping.
7. Study the dielectric behaviour and dissipation factor of glass ceramic samples as a function of frequency and temperature.

3. EXPERIMENTAL PROCEDURE

PREPARATION OF $[(\text{Ba}_{0.3}, \text{Sr}_{0.7})\text{O}.\text{TiO}_2]\text{--}[\text{2SiO}_2\text{--B}_2\text{O}_3]\text{--}[\text{K}_2\text{O}]$ (SBT) BASE GLASS

The composition of base glass was $[(\text{Ba}_{0.3}, \text{Sr}_{0.7})\text{O}.\text{TiO}_2]\text{--}[\text{2SiO}_2\text{--B}_2\text{O}_3]\text{--}[\text{K}_2\text{O}]$. The batch was prepared by mixing the stoichiometric amount of chemicals listed in **Table 3.1** with the help of acetone as mixing media (for homogenous mixing). Two batches of the glass, 75gm each were made. The glass samples were prepared by melt quench method. The raw materials were mixed in an agate mortar and melted in a platinum crucible at 1350°C inside a pit furnace. The liquid melt was quenched either on a pre-heated graphite plate or quenched onto a steel plate at room temperature.

PREPARATION OF 0.1 mol% La_2O_3 DOPED $[(\text{Ba}_{0.3}, \text{Sr}_{0.7}).\text{O.TiO}_2]-[\text{2SiO}_2-\text{B}_2\text{O}_3]-[\text{K}_2\text{O}]$ (SBT) GLASS

The composition of base glass was $[(\text{Ba}_{0.3}, \text{Sr}_{0.7}).\text{O.TiO}_2]-[\text{2SiO}_2-\text{B}_2\text{O}_3]-[\text{K}_2\text{O}]-0.1[\text{La}_2\text{O}_3]$. The batch was prepared by mixing the compounds with the help of acetone mixing media (for homogenous mixing). This time only one batch of the glass, 75gm was made. The batch of glass is prepared by following the process of melt quench method. The temperature at which the molten glass is taken out of the furnace and casted is 1350°C . The step followed here is the molten glass is quenched directly to the room temperature. The temperature raising in the furnace is pre calculated which includes a soaking time of 1hr at 1350°C . This method is followed to make the glass homogeneously melted. After the glass sample is collected then different characterizations were done.

GLASS FORMATION

The glass is made by melt quenching process where the components of glass is poured into an alumina crucible. The entire glass sample was poured into it and was heated from the room temperature. The heat treatment schedule followed here it pre-calculated. The furnace in which the glass was melted is known to be raising hearth furnace. The temperature at which we take the glass samples out of the furnace is 1350°C . After melting of the glass sample the glass is annealed for approximately 45 minutes and then annealing is done in order to remove the stress from the glass. The annealing should be done at lower temperature. The sample is collected after being cooled. Appropriate precautions should be taken while transferring the molten glass at 1350°C and care should also be taken while opening the furnace at 1350°C so that the refractory in the furnace should not get damaged due to thermal shock resistance.

Table 3.1: Raw material used for the preparation of glass samples

Sl. No.	Compound Name	Percentage Purity	Company Name
1	SiO ₂	99.8 %	TRL Belpahar
2	BaCO ₃	97 %	Merck
3	K ₂ CO ₃	99.9 %	Merck
4	H ₃ BO ₃	99.5 %	Merck
5	TiO ₂	≥ 99 %	Merck
6	La ₂ O ₃	99.9 %	Lova Chemie
7	SrCO ₃	99 %	S.D. Fine chemical Ltd.

PREPARATION OF GLASS CERAMICS

After the glass samples were collected some part of the sample is grounded into powder. Then the glass powder is characterized through Differential Thermal Calorimeter (DSC). The information we get from the DSC curve is the T_g (glass transition temperature), T_{C1} and T_{C2} (where T_{C1} and T_{C2} are crystallization temperature). Depending upon the information we get from the DSC curve glass ceramization procedure is followed by further heat treatment method. The samples were kept on an alumina base plate and according to the respective temperatures the samples were heat treated. These samples were heat treated on the basis of the heat treatment schedule.

DIFFERENTIAL SCANNING CALORIMETERY (DSC) STUDY

Differential Scanning Calorimetry, DSC, is the next step to be followed. For the study of the DSC a small part of the sample is taken and is grounded to very fine powders. The sample is now ready for the Differential Scanning Calorimetry (DSC). The powdered sample weighing approximately 100mg is now poured into the alumina crucible with the help of tweezer and spatula. The crucible is now loaded into the DSC equipment (Netzsch, Germany, STA449C/4/MFC/G) and the measurements were taken from room temperature to 700°C with a heating rate of 10°Cmin⁻¹. For glasses, the onset of glass transition can be estimated from the DSC thermogram which shows an endothermic signal while crystallization event exhibits an

exothermic signal. The DSC also gives the onset of crystallization temperature (T_x) and the crystallization temperature through the exothermic peaks.

DENSITY MEASUREMENT

The density of glass was determined by placing a glass sample into suspension in distilled water solution. The density measurement is done through immersing all the samples in the distilled water and treating the entire system with heat or vacuum. But before immersion the dry weight of the samples were measured. After few hours the samples were taken out of the systems and there suspended weight and soaked weight were measured.

$$\rho = \left[\frac{D}{(W-S)} \right]$$

Where, ρ is the density of the glass in gm/cc.

D Dry weight of the sample,

W Soaked weight of the sample,

S Suspended weight of sample when suspended in liquid.

PHASE ANALYSIS USING X-RAY DIFFRACTION

For the XRD analysis a very small part of the sample is chosen and it is grounded to very fine powders using agate and mortar. The powdered sample is now spread over the sample holder and then the XRD (Rigaku Japan/Ultima-IV) of the sample is performed having the 2θ value from $10-70^\circ$ using the step size 0.05 and CuK_α radiation. From the XRD patterns the primary phase and the secondary phase formed are determined.

FOURIER TRANSFORM INFRARED SPECTROSCOPY (FTIR) STUDY

The Fourier transform infrared spectroscopy (FTIR) was performed using PerkinElmer Spectrum Two (model number 95277) spectrometer between $4000 \sim 450 \text{ cm}^{-1}$. The FTIR pellet sample was prepared by mixing the powder with the KBr (:10 wt.% ratio) followed by hydraulic pressing. Reference pellet of KBr was also prepared in order to cancel out the FTIR spectra of KBr from the desired glass sample. The FTIR spectra is helpful to identify the bonds

present in the glass. The FTIR peaks present in the scan due to the different stretching and relaxation of the bonds present in the glass. The model and serial number of the equipment used is instrument model spectrum two instrument serial number 95277.

FIELD EMISSION SCANNING ELECTRON MICROSCOPE (FESEM) STUDY

Prior to FESEM the samples were properly polished using sand grit paper followed by diamond polish in order to get the mirror-like finish on its surface. The samples were then gold coated in order to avoid charging during FESEM study. Microstructural analysis of the glass ceramic samples were performed at 30kV using a Field Emission Scanning Electron Microscope (NOVA NanoSEM/FEI).

DIELECTRIC MEASUREMENT

The glass ceramic samples were made to desired shape. Surfaces of the glass ceramic samples were polished using sand papers (grit 240, grit 320) followed by polishing using emery paper (grit 600, grit 1200) and diamond paste (3 μ m) on a lapped cloth to get a mirror-like finish. The desired thickness of the sample should be ~1mm. The electrodes were made by applying silver paste on both the surfaces of the samples. The samples were then cured at 600 $^{\circ}$ C for 1hour. The samples were now ready for the dielectric measurements. The dielectric parameters like capacitance (C), dielectric loss or dissipation factor ($\tan\delta$ or D) and conductance (G) were measured as a function of frequency and temperature in a locally fabricated platinum sample holder using a HIOKI 3532-50 LCR High Tester. The entire system is prevented from any disturbances as it was shielded with metallic jacket. The measurements were carried out in the frequency range 100Hz-1MHz and temperature range from 27-250 $^{\circ}$ C. Measurements were taken at an interval of 10 $^{\circ}$ C at steady temperatures.

Dielectric constant (ϵ_r) was calculated from capacitance (C) using the relation;

$$\epsilon_r = C \cdot t / (\epsilon_0 \cdot A)$$

Where C is capacitance, ϵ_0 is the permittivity of free space ($\epsilon_0=8.854 \times 10^{-12}$ F/m), A and t are area and thickness of the sample in square meter and meter respectively.

4. RESULTS AND DISCUSSION

PHASE ANALYSIS OF GLASS SAMPLES

SBT base glasses quenched through the techniques like pre-heated graphite plate and air quenched were analysed. 0.1 mol % La_2O_3 doped SBT glass quenched in air is also analysed. After the three glass samples were prepared a small part of it is grounded to fine powders and X-ray diffraction is done to confirm that it is a glass. **Figure 4.1-4.3** shows the XRD plot of each samples having the compositions $[(\text{Ba}_{0.3}\text{Sr}_{0.7}).\text{O.TiO}_2]-[2\text{SiO}_2-\text{B}_2\text{O}_3]-[\text{K}_2\text{O}]$ preheated plate graphite plate quenched, $[(\text{Ba}_{0.3}\text{Sr}_{0.7}).\text{O.TiO}_2]-[2\text{SiO}_2-\text{B}_2\text{O}_3]-[\text{K}_2\text{O}]$ quenched at room temperature and the doped glass $[(\text{Ba}_{0.3}\text{Sr}_{0.7}).\text{O.TiO}_2]-[2\text{SiO}_2-\text{B}_2\text{O}_3]-[\text{K}_2\text{O}]-0.1[\text{La}_2\text{O}_3]$ also quenched at room temperature respectively. The XRD curve of all the glasses shows a very broad peak which concludes that the material is glass. The broad peak that is observed in each graph is due to the local periodicity.

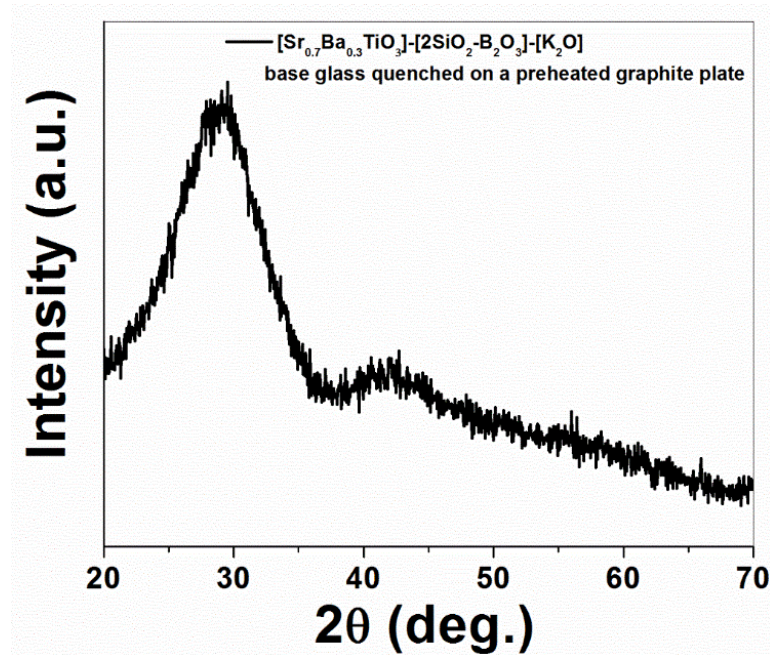


Figure 4.1 XRD pattern of $[(\text{Ba}_{0.3}, \text{Sr}_{0.7}).\text{O.TiO}_2]-[2\text{SiO}_2-\text{B}_2\text{O}_3]-[\text{K}_2\text{O}]$ glass quenched on a preheated graphite plate

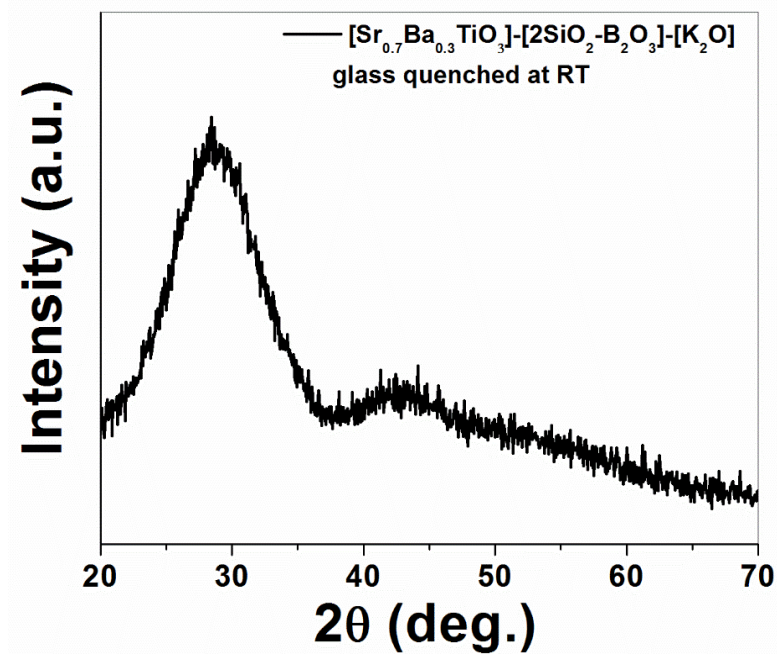


Figure 4.2 XRD pattern of $[(\text{Ba}_{0.3}\text{Sr}_{0.7}).\text{O.TiO}_2]\text{-}[2\text{SiO}_2\text{-B}_2\text{O}_3]\text{-}[\text{K}_2\text{O}]$ glass quenched at room temperature

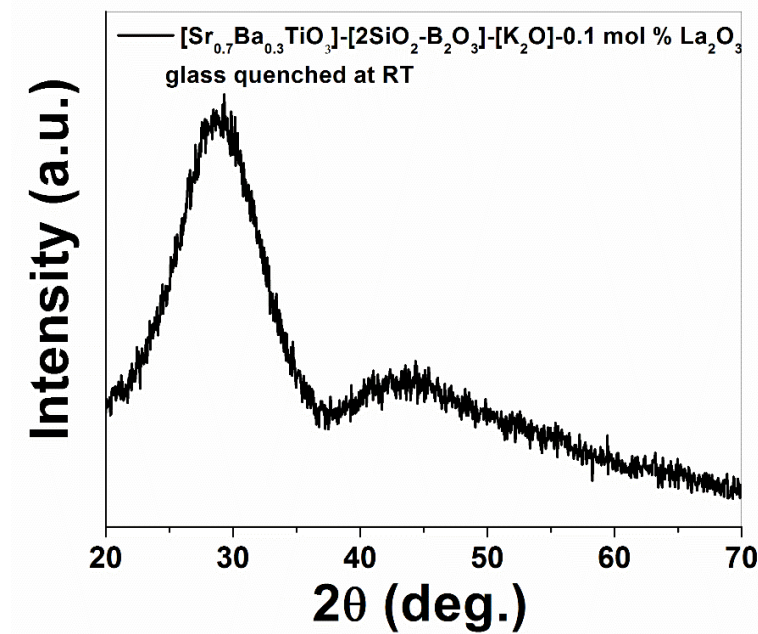


Figure 4.3 XRD pattern of $[(\text{Ba}_{0.3}\text{Sr}_{0.7}).\text{O.TiO}_2]\text{-}[2\text{SiO}_2\text{-B}_2\text{O}_3]\text{-}[\text{K}_2\text{O}]\text{-}0.1\text{mol \%}[\text{La}_2\text{O}_3]$ glass quenched at room temperature

FTIR SPECTRA OF GLASS SAMPLES

The FTIR spectrum for the SBT base glass and 0.1 mol % La_2O_3 doped SBT glass is shown in **Figure 4.4 (a) and (b)**. The peaks of the infrared spectroscopy are listed in the **Table**

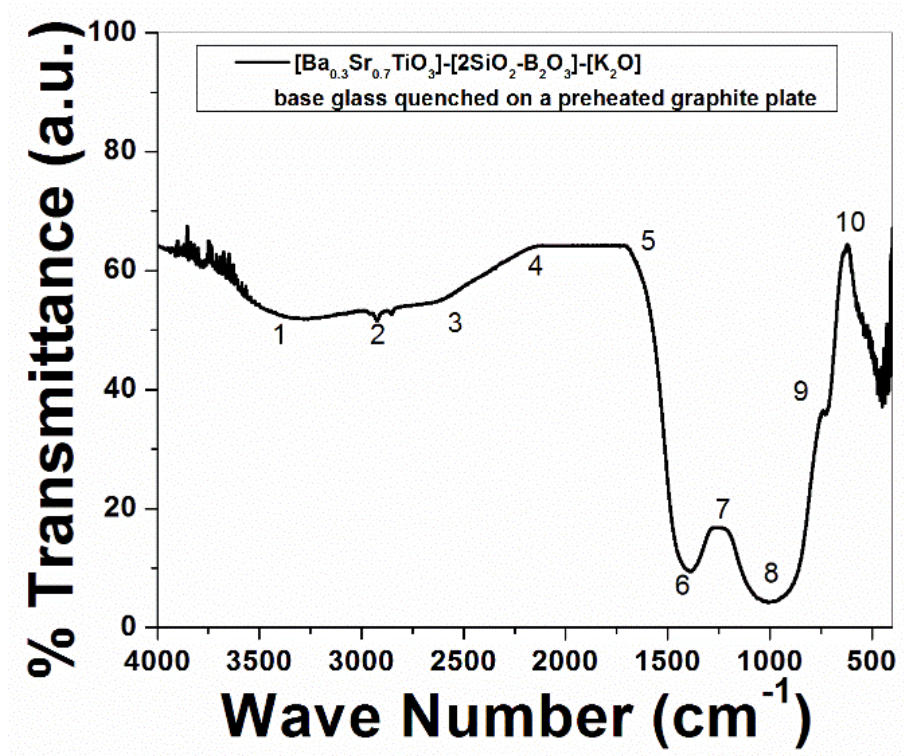
4.1 and 4.2. The FTIR spectra for these glasses generally consist of broad and diffuse bands in the region 450-4000 cm^{-1} . Each broad peak in the **Figure 4.4(a-b)** gives an indication of one or more vibrational contributions from the group of ions. These bands are further influenced by the ratio of Ba/Sr present in the glass. The transmission band in the wave number range 3436–3456 cm^{-1} observed due to the molecular water present inside the glassy matrix [12]. The transmission band in the wave range 2340 – 2927 cm^{-1} gives an indication about the hydrogen bonding in glassy network and these band are not affected by the variations of Ba/Sr ratio [13-15]. Glass samples showing diffused adsorption bands in the range of wave number 2340 – 2365 cm^{-1} . A doublet splitting was observed in this band and is also attributed to –OH bonding vibrations. These are formed at nonbridging oxygen sites. These –OH groups may be present due to the KBr pellet technique [16]. Few absorption bands are also present in the range 1275 – 1739 cm^{-1} . In this wavenumber range peaks are observed due to the asymmetric stretching relaxation of B-O bonds of trigonal BO_3 units [17,18]. At 983 cm^{-1} wavenumber it attributes to the stretching and vibration of B-O-Si linkage [19]. From 707 – 719 cm^{-1} wavenumber range the peaks are due to the diborate (B-O-B) link found in the borate glassy network [20]. At 977 cm^{-1} wavenumber the peak is due to the B-O stretching in orthorombhic units. Similarly at 829 cm^{-1} wavenumber it is attributed due to the B-O-B stretching pyroborate units [21,22]

Table 4.1 List of FTIR peaks observed for SBT base glass

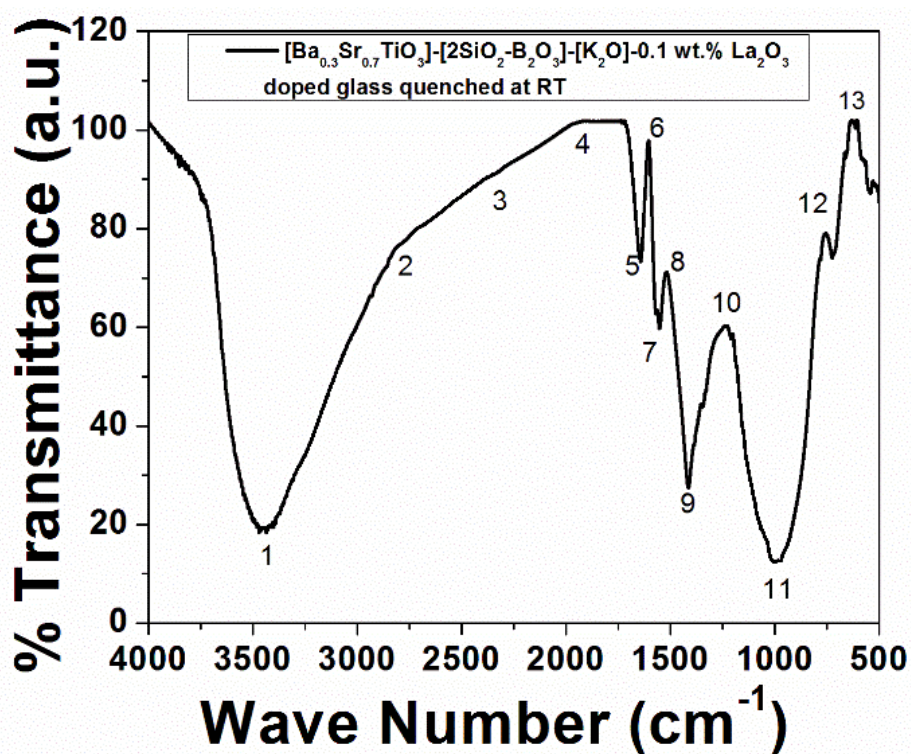
Glass Sample	Peak number	Wave number (cm^{-1})
SBT base glass	1	3448.83
	2	2928.23
	3	2591.30
	4	2353.86
	5	1752.42
	6	1408.32
	7	1242.74
	8	977.48
	9	711.05
	10	676.54

Table 4.2 List of FTIR peaks observed for doped glass

Glass Sample	Peak number	Wave number (cm ⁻¹)
0.1 mol % La ₂ O ₃ doped SBT glass	1	3446.51
	2	2925.03
	3	2572.54
	4	1960.86
	5	1733.30
	6	1612.47
	7	1556.40
	8	1514.75
	9	1417.04
	10	1228.83
	11	981.35
	12	754.69
	13	636.15



(a)



(b)

Figure 4.4 FTIR spectra of (a) SBT base glass and (b) 0.1 mol % La_2O_3 doped SBT glass

DSC STUDY OF GLASS SAMPLES

The DSC study of all glass samples were done from room temperature to 700°C at a heating rate of 10°Cmin^{-1} . The DSC trace of different base glass samples in the system $[(\text{Ba}_{0.3}, \text{Sr}_{0.7}).\text{O}.\text{TiO}_2]-[\text{2SiO}_2-\text{B}_2\text{O}_3]-[\text{K}_2\text{O}]$ quenched through different methods like water quenching, quenching at room temperature and pre-heated graphite plate are shown in **Figure 4.5 - 4.6**. The DSC trace of the pure strontium glass with the nominal composition $[\text{SrTiO}_3]-[\text{2SiO}_2-\text{B}_2\text{O}_3]-[\text{K}_2\text{O}]$ is presented in the **Figure 4.7**. The DSC trace of the 0.1 mol % La_2O_3 doped into the base glass system i.e. $[(\text{Ba}_{0.3}, \text{Sr}_{0.7}).\text{O}.\text{TiO}_2]-[\text{2SiO}_2-\text{B}_2\text{O}_3]-[\text{K}_2\text{O}]-0.1 \text{ mol } \% [\text{La}_2\text{O}_3]$ is also shown in the **Figure 4.8**.

From the **Figure 4.5** the sample is pre heated plate quenched base glass from the graph we could see that the glass shows an exothermic peak at 587°C . Another peak from the curve could be seen at 685°C . From the **Figure 4.6** we could very well observe that the glass transition

temperature (T_g) is 325°C . The onset of crystallization temperature is found to be around 495°C . So, a temperature between 495°C to 587°C is chosen for making of glass ceramics because below 495°C no crystallization will be observed and after 587°C the entire sample will be crystallized. As we require partial crystallization of glass where both glass and crystals will be present and they show the respective properties. Increasing the dwelling time at crystallization temperature will increase the crystal size. The onset of crystallization temperature is mentioned to be T_x . the stability factor of a glass can be calculated from the formula $T_x - T_g$. In preheated plate quenched base glass the stability factor is calculated to be around 170°C .

From the **Figure 4.7** the sample is air quenched base glass having the same glass system as preheated plate quenched base glass. From the graph we could see that the glass shows a peak at 581°C . From the **Figure 4.7** we could very well observe that the glass transition temperature (T_g) is 330°C . The onset of crystallization temperature is found to be around 521°C . So, a temperature between 521°C to 581°C is chosen for making of glass ceramics because below 521°C no crystallization will be there and after 581°C the entire sample will be crystallized. As we require partial crystallization of glass where both glass and crystals will be present and they show the respective properties. Increasing the dwelling time at ceramization temperature will increase the crystal size. The onset of crystallization temperature is mentioned to be T_x . the stability factor of a glass can be calculated from the formula $T_x - T_g$. In preheated plate quenched base glass the stability factor is calculated to be around 191°C .

From the **Figure 4.8** the sample is pure strontium base glass from the graph we could see that the glass shows only one peak at 593°C . From the **Figure 4.8** we could very well observe that the glass transition temperature (T_g) is 325°C . The onset of crystallization temperature is found to be around 575°C . So, a temperature between 575°C to 593°C was chosen for making of glass ceramics because below 575°C no crystallization will be there and

after 593⁰C the entire sample will be crystallized. As it requires partial crystallization of glass where both glass and crystals will be present and they show the respective properties. Increasing the dwelling time at ceramization temperature will increase the crystal size. The onset of crystallization temperature is mentioned to be T_x . the stability factor of a glass can be calculated from the formula $T_x - T_g$. In preheated plate quenched base glass the stability factor is calculated to be around 250⁰C.

From the **Figure 4.9** the sample is 0.1 mol % La₂O₃ glass from the graph we could see that the glass shows only one peak at 601⁰C. From the **Figure 4.9** we could very well observe that the glass transition temperature (T_g) is 320⁰C. The onset of crystallization temperature is found to be around 580⁰C. So, a temperature between 575⁰C to 593⁰C is chosen for making of glass ceramics because below 580⁰C no crystallization will be there and after 601⁰C the entire sample will be crystallized. As it requires partial crystallization of glass where both glass and crystals will be present and they show the respective properties. Increasing the dwelling time at ceramization temperature will increase the crystal size. The onset of crystallization temperature is mentioned to be T_x . the stability factor of a glass can be calculated from the formula $T_x - T_g$. In preheated plate quenched base glass the stability factor is calculated to be around 260⁰C.

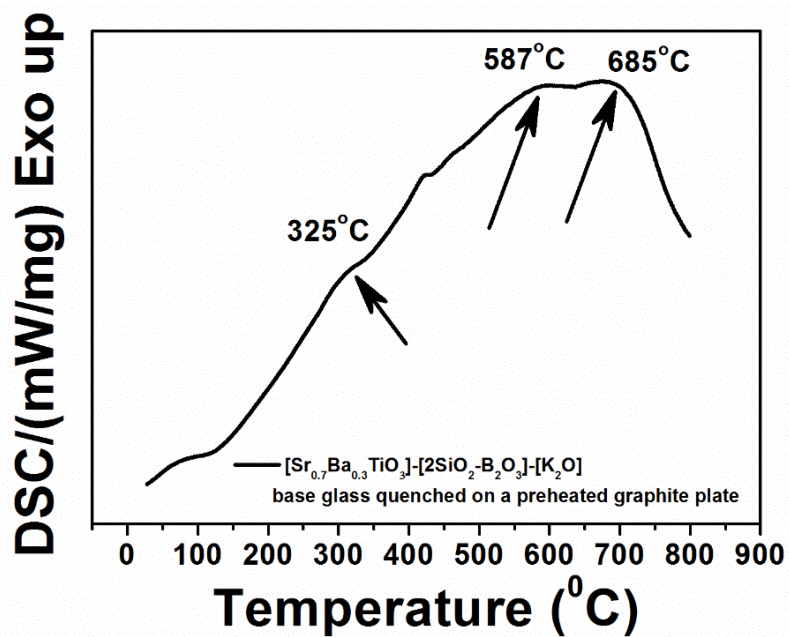


Figure 4.5 DSC scan from room temperature to 800°C of pre-heated plate quench base glass sample

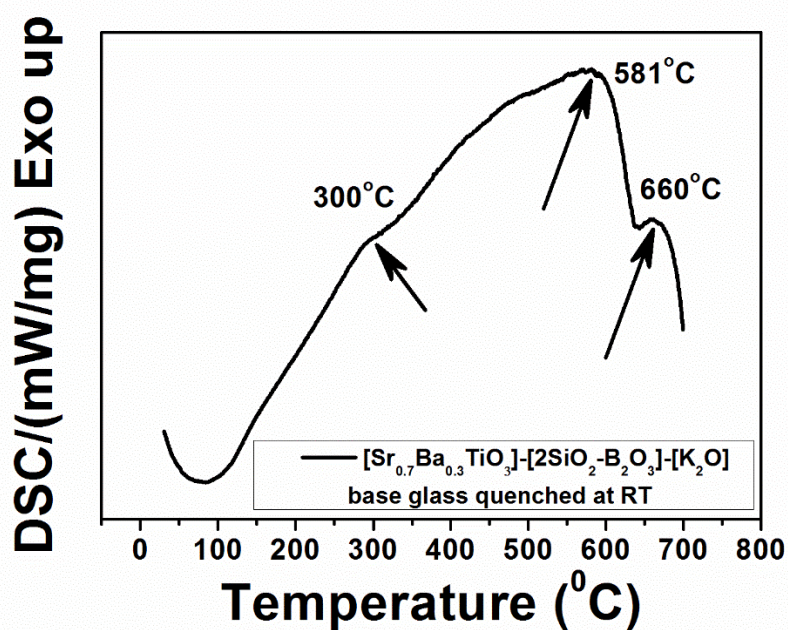


Figure 4.6 DSC study of from room temperature to 700°C of air quenched base glass sample

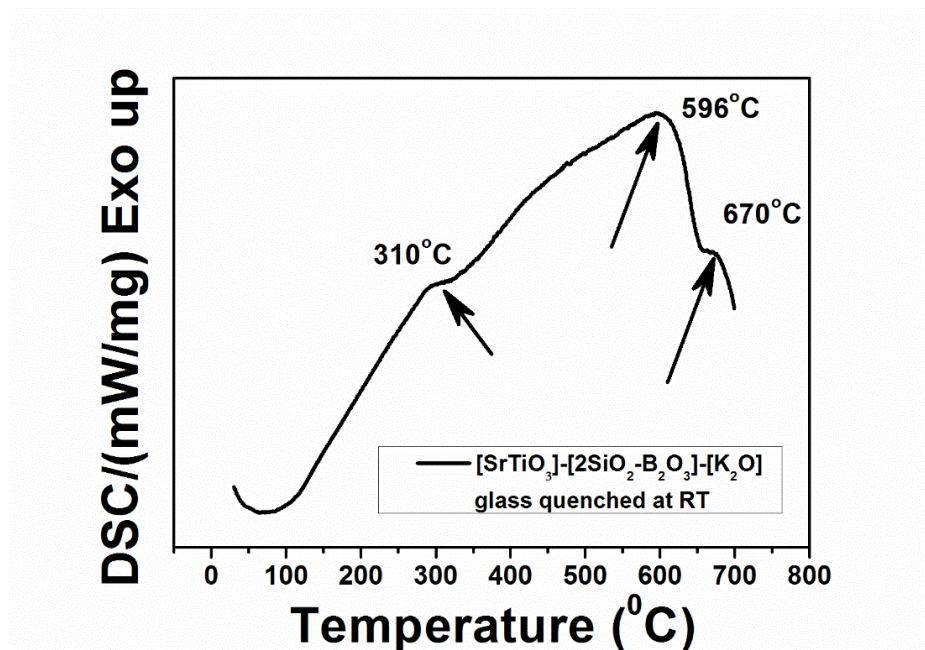


Figure 4.7 DSC study from room temperature to 800°C of pure strontium base glass sample

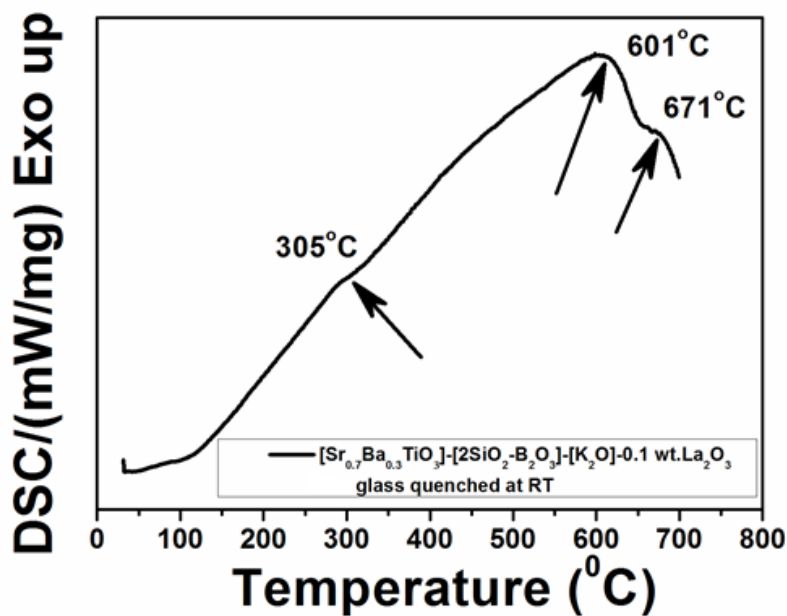


Figure 4.8 DSC study from room temperature to 700°C of 0.1 mol % La_2O_3 doped glass sample

DENSITY MEASUREMENT

The density studies of the four samples were done. The two of them are glass samples which are SBT base glass and 0.1 mol % La_2O_3 doped SBT glass. The other two samples are

the crystallized ones of the above mentioned samples. From the **Table 4.3** and **4.4** it could be very well observed that the glass ceramic samples are having slightly higher bulk density than those of glass samples.

The density of the glass samples are slightly lower in comparison to glass ceramic samples as they have been transformed from an amorphous structure to a crystalline structure. The growth and formation of crystals in-between the samples increases the density of the glass. With the doping of La_2O_3 the density of the sample increases. With the increase of the dwelling time the crystal size increases which results in the increase of the density of the glass ceramic.

Table 4.3. Density measurement of the glass samples before crystallization

Glass samples	Dry weight (D) gm	Suspended weight (S) gm	Soaked weight (W) gm	Bulk density = $D/(W-S)$	Average
Base glass (quenched at high temperature)	1. 14.7408	1. 9.7435	1. 14.7462	1. 2.95	2.91 g/cc ± 0.03
	2. 1.3429	2. 0.8912	2. 1.3429	2. 2.91	
	3. 1.4216	3. 0.9362	3. 1.4283	3. 2.89	
Doped glass (quenched at room temperature)	1. 2.2826	1. 1.5478	1. 2.2842	1. 3.05	3.04 g/cc ± 0.007
	2. 2.1172	2. 1.4359	2. 2.1181	2. 3.03	
	3. 2.1346	3. 1.4613	3. 2.1392	3. 3.04	

Table 4.4. Density measurement of the glass ceramic samples after crystallization

Glass samples	Dry weight (D) gm	Suspended weight (S) gm	Soaked weight (W) gm	Bulk density = $D/(W-S)$	Average
Base glass (quenched at high room temperature)	1. 1.0337	1. 0.6855	1. 1.0342	1. 2.96	2.94 g/cc ± 0.015
	2. 2.6199	2. 1.7340	2. 2.6199	2. 2.95	
	3. 1.1154	3. 0.7321	3. 1.1164	3. 2.93	
Doped glass (quenched at room temperature)	1. 1.5454	1. 1.0525	1. 1.5497	1. 3.11	3.11 g/cc ± 0.012
	2. 1.8748	2. 1.2752	2. 1.8749	2. 3.12	
	3. 1.6394	3. 1.1083	3. 1.6346	3. 3.09	

PHASE ANALYSIS OF GLASS CERAMIC SAMPLES

SBT base glass ceramics quenched through the techniques like pre-heated graphite plate and air quenched while making were analysed. 0.1 mol % La_2O_3 doped SBT glass ceramics quenched in air while making glass is also analysed. The composition of the three glass samples are $[(\text{Ba}_{0.3}, \text{Sr}_{0.7}).\text{O.TiO}_2]-[\text{2SiO}_2-\text{B}_2\text{O}_3]-[\text{K}_2\text{O}]$ quenched on preheated plate graphite plate, $[(\text{Ba}_{0.3}, \text{Sr}_{0.7}).\text{O.TiO}_2]-[\text{2SiO}_2-\text{B}_2\text{O}_3]-[\text{K}_2\text{O}]$ quenched at room temperature and the doped glass $[(\text{Ba}_{0.3}\text{Sr}_{0.7}).\text{O.TiO}_2]-[\text{2SiO}_2-\text{B}_2\text{O}_3]-[\text{K}_2\text{O}]-0.1[\text{La}_2\text{O}_3]$ also quenched at room temperature respectively.

After controlled heat treatment the glasses were crystallized and had turned from glass to glass ceramics. The glass samples had turned to glass ceramics is confirmed only through XRD observation. **Figure 4.9-4.11** shows the XRD plot of each glass ceramic samples having the compositions $[(\text{Ba}_{0.3}, \text{Sr}_{0.7}).\text{O.TiO}_2]-[\text{2SiO}_2-\text{B}_2\text{O}_3]-[\text{K}_2\text{O}]$ preheated plate graphite plate quenched, $[(\text{Ba}_{0.3}, \text{Sr}_{0.7}).\text{O.TiO}_2]-[\text{2SiO}_2-\text{B}_2\text{O}_3]-[\text{K}_2\text{O}]$ quenched at room temperature and the doped glass ceramics $[(\text{Ba}_{0.3}\text{Sr}_{0.7}).\text{O.TiO}_2]-[\text{2SiO}_2-\text{B}_2\text{O}_3]-[\text{K}_2\text{O}]-0.1[\text{La}_2\text{O}_3]$ also quenched at room temperature respectively. In the **Figure 4.9** SBT base glass composition preheated graphite plate quenched the patterns shows that the primary phase formed is $\text{Sr}_{0.744}\text{Ba}_{0.2056}\text{TiO}_3$ and the secondary phase formed are SiO_2 and Ba_3SiO_5 and it is confirmed through JCPDS file. The major crystalline phase, SBT exists in tetragonal crystal structure. This major crystalline phase forms perovskite structure. The Lattice parameter(s) were calculated by least-square technique. Calculated Lattice parameter(s) of the sample [$a = 0.39063 \text{ nm}$ and unit cell volume $= 59.61 \times 10^{-3} \text{ nm}^3$] matched quite well with the standard lattice cell parameter(s) [$a = 0.39250 \text{ nm}$ and unit cell volume $= 60.47 \times 10^{-3} \text{ nm}^3$] of SrBaTiO_3 phase. However in case of SBT base glass quenched at room temperature the patterns shown in the **Figure-4.10** confirms that the primary phase formed here is $\text{Sr}_2\text{TiSi}_2\text{O}_8$ and the secondary phase formed here is silica (SiO_2). In this case perovskite structure is not formed and this was also confirmed through JCPDS file.

The required phase has not formed since it might require much higher temperature for its formation. The energy barrier in this case might have been higher in comparison to the preheated graphite plate quenched glass ceramics. In the **Figure 4.11** the XRD patterns confirm that the primary phase formed after crystallization is $\text{Sr}_{0.9}\text{La}_{0.1}\text{TiO}_3$ which is the required phase along with the primary phase the secondary phases observed are SiO_2 and Ba_3SiO_5 and it is also confirmed through JCPDS file. The major crystalline phase, 0.1 mol % La_2O_3 SBT exists in tetragonal crystal structure. This major crystalline phase forms perovskite structure. Lattice parameter(s) were calculated by least-square technique. Calculated Lattice parameter(s) of the sample [$a = 0.39150$ nm and unit cell volume = $60.01 \times 10^{-3} \text{ nm}^3$] matched quite well with the standard lattice cell parameter(s) [$a = 0.39111$ nm and unit cell volume = $59.83 \times 10^{-3} \text{ nm}^3$] of $\text{Sr}_{0.9}\text{La}_{0.1}\text{TiO}_3$ phase. It can be seen that with the doping of La_2O_3 in the SBT glass, La_2O_3 promotes the crystallization and influences the degree of crystallinity. The substitution of La^{3+} ions into the Sr^{2+} sites enhanced the stability of the perovskite structure because of a higher bond strength associated with the La-O compared to Ba-O bonds. Hence the formation of stronger bonds would certainly suppress the formation of intrinsic defects [23].

From XRD data there is an indication that the doped glass gets crystallized at lower temperature than the SBT base glass as the crystallized graph of SBT base glass is the sample is crystallized at 780°C for 3hrs whereas the doped SBT glass gets crystallized at 750°C for 3hrs. Hence La_2O_3 here acts as a nucleating agent.

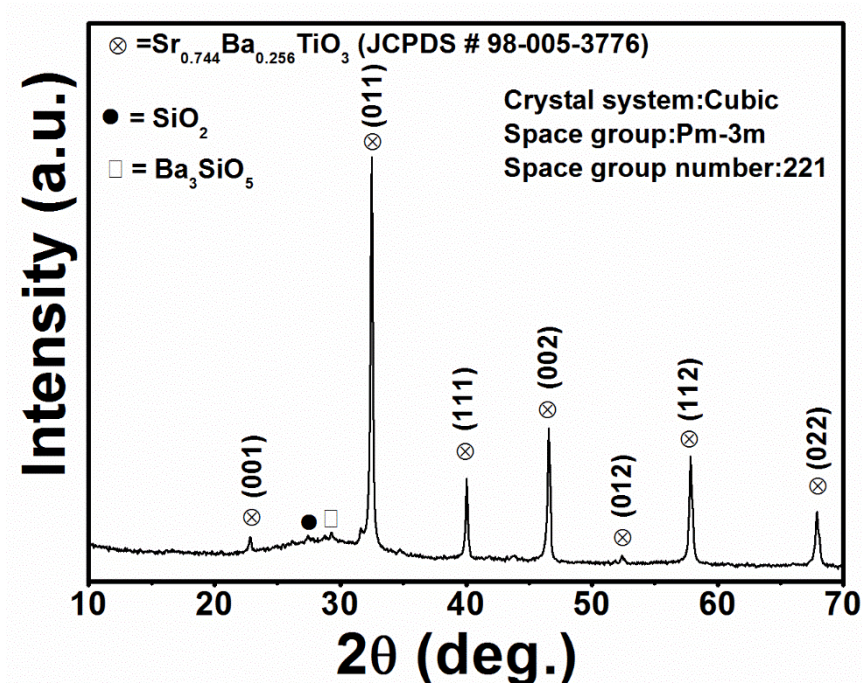


Figure 4.9 XRD pattern of $[(\text{Ba}_{0.3}, \text{Sr}_{0.7}).\text{O.TiO}_2]-[2\text{SiO}_2-\text{B}_2\text{O}_3]-[\text{K}_2\text{O}]$ glass ceramic sample crystallized at 780°C for 3h in air

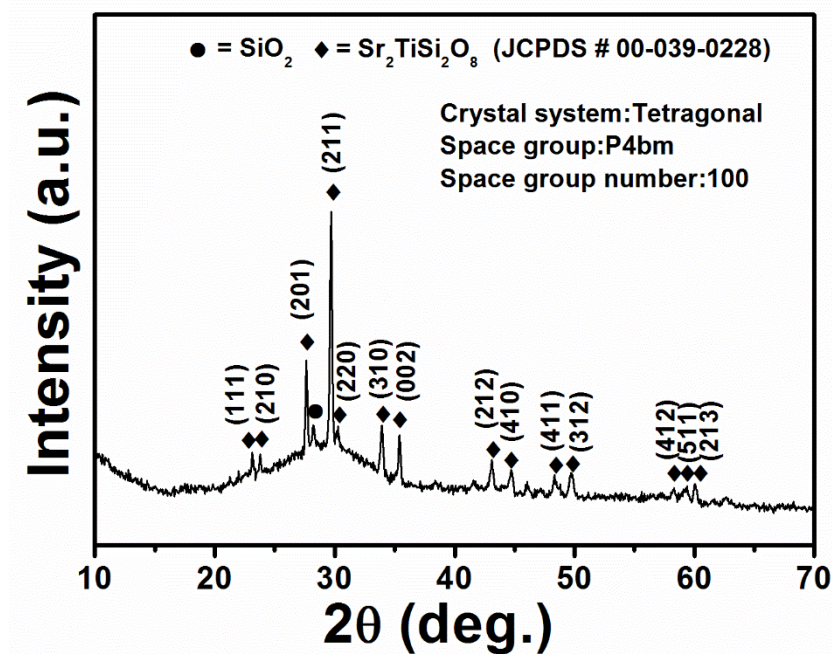


Figure 4.10 XRD pattern of $[(\text{Ba}_{0.3}, \text{Sr}_{0.7}).\text{O.TiO}_2]-[2\text{SiO}_2-\text{B}_2\text{O}_3]-[\text{K}_2\text{O}]$ glass ceramic sample crystallized at 780°C for 3h in air

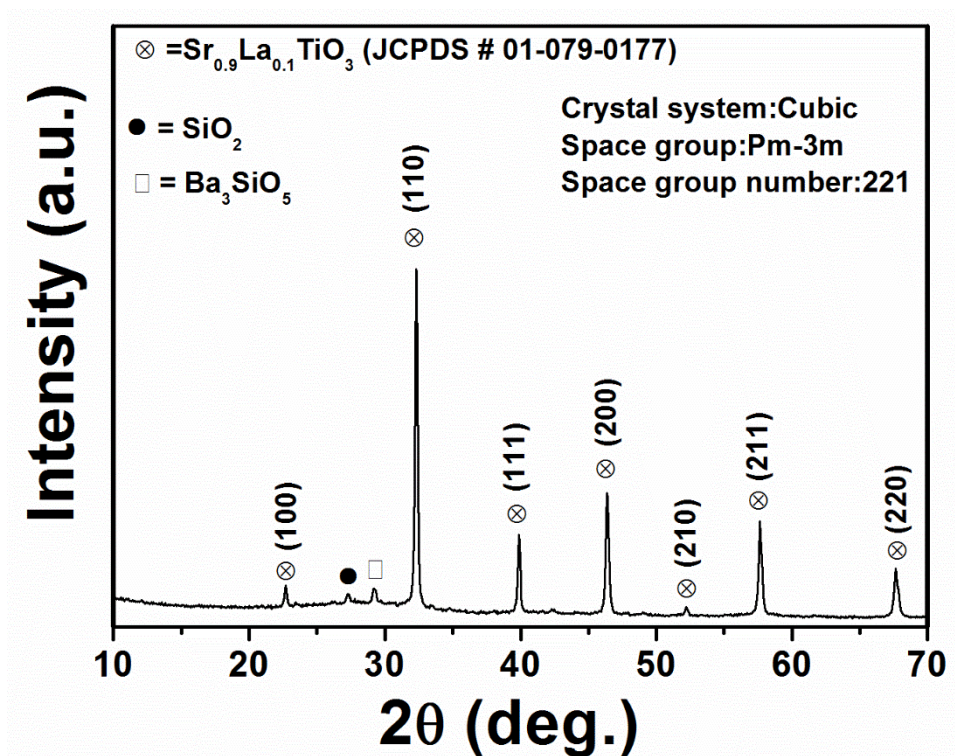


Figure 4.11 XRD pattern of [(Ba_{0.3}, Sr_{0.7}).O.TiO₂]-[2SiO₂-B₂O₃]-[K₂O]-0.1 mol % [La₂O₃] glass ceramic crystallized at 750°C for 3h in air

MICROSTRUCTURAL ANALYSIS OF GLASS CERAMIC SAMPLES

The surface morphology of SBT base glass ceramic having the composition [(Ba_{0.3}, Sr_{0.7}).O.TiO₂]-[2SiO₂-B₂O₃]-[K₂O] and also the surface morphology of 0.1 mol % La₂O₃ doped SBT glass ceramics having the composition [(Ba_{0.3}, Sr_{0.7}).O.TiO₂]-[2SiO₂-B₂O₃]-[K₂O]-0.1[La₂O₃] were observed. SEM showed the detailed microstructural morphology analysis of the samples. Elemental X-Ray mapping results were also obtained which shows the distribution of the all the elements present in the microstructure. Energy Dispersive Spectroscopy (EDS) results obtained shows the quantitative analysis of the microstructures present in the samples.

The **Figure 4.12** shows the surface morphology of the SBT base glass ceramic. The morphology shows there are two types of crystals formed within it one of them is flower-like and the other one is needle-like. The elemental X-ray mapping and EDS gives us the detailed composition of the both flower-like and needle-like crystals and are presented in **Figure 4.13-4.15** and from these data we could conclude that the flower-like crystals are rich in strontium

as $\text{Sr}^{2+}/\text{Ti}^{4+}$ ratio ~ 0.8 matches with the ratio of $\text{Sr}^{2+}/\text{Ti}^{4+}$ (0.75) in the $\text{Sr}_{0.744}\text{Ba}_{0.256}\text{TiO}_3$ composition. So we could very well conclude that the major phase formed in the flower like crystal structure is $\text{Sr}_{0.744}\text{Ba}_{0.256}\text{TiO}_3$. However the needle like crystals formed may form barium silicate ($\text{Ba}_3\text{Si}_2\text{O}_8$) phase and this is also known from the EDS analysis which is presented in the **Figure 4.14**. The sample has borosilicate matrix may also be concluded.

The **Figure 4.16** shows the surface morphology of the 0.1 mol % La_2O_3 doped SBT glass ceramics. The morphological analysis of the doped glass shows blocky irregular shaped interconnected crystals are observed throughout the microstructure after controlled crystallization. The elemental X-ray mapping and EDS gives us the detailed composition of the blocky irregular shaped interconnected like crystals and are presented in **Figure 4.17-4.18** and from these data we could conclude that blocky irregular shaped interconnected like crystals are rich in strontium in the $\text{Sr}_{0.9}\text{La}_{0.1}\text{TiO}_3$ composition. So we could very well conclude that the major phase formed in the blocky irregular shaped interconnected like crystal structure is $\text{Sr}_{0.9}\text{La}_{0.1}\text{TiO}_3$. The EDS analysis also shows that some amount of barium is also present in the blocky irregular shaped interconnected like crystal structure. The matrix in major may have the borosilicate composition.

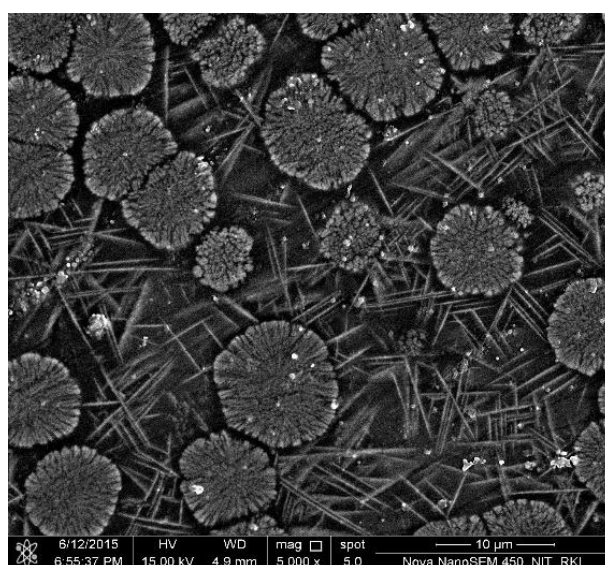


Figure 4.12 SEM image of SBT base glass ceramic

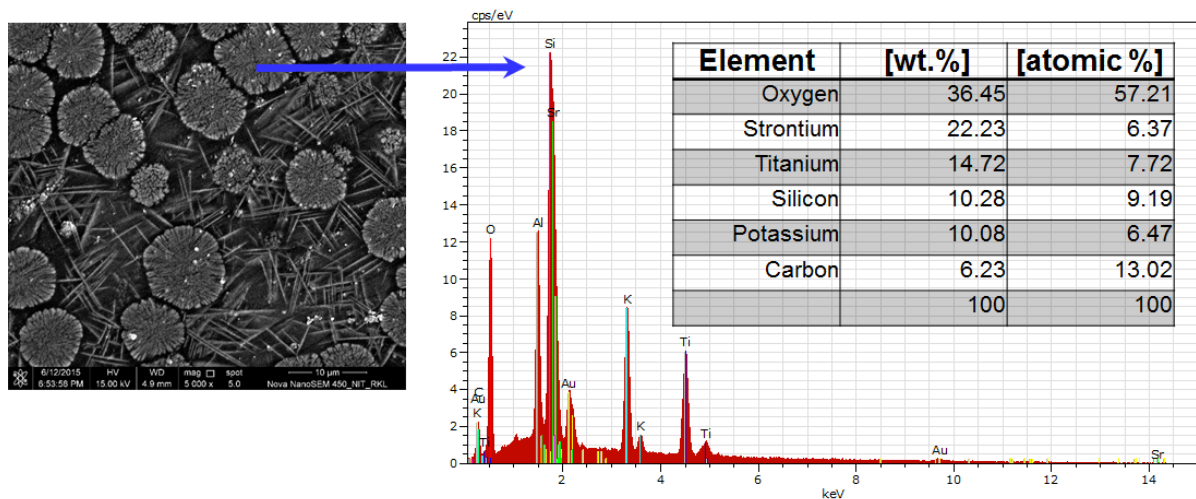


Figure 4.13 EDS analysis of flower like crystal found in the microstructure

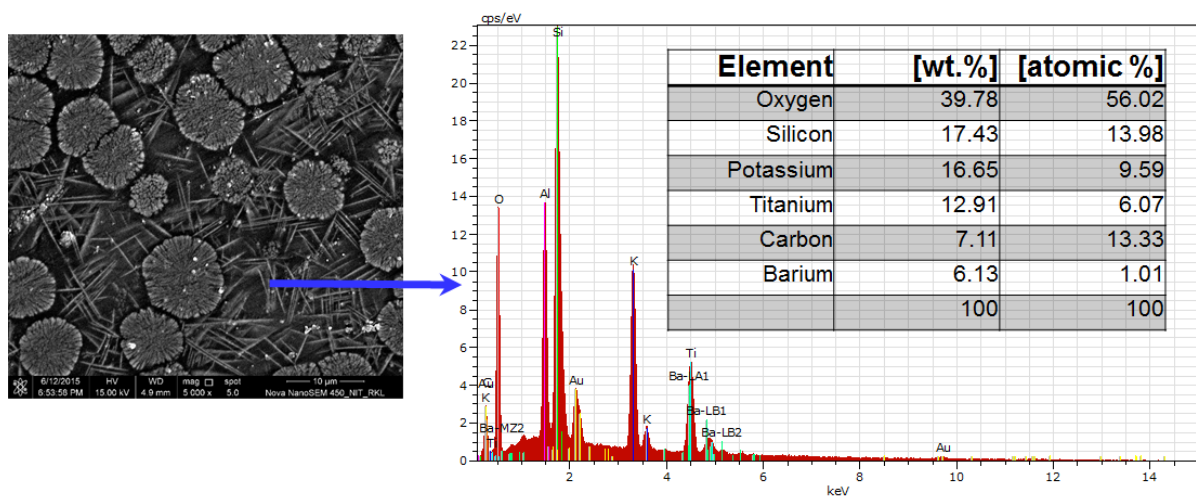


Figure 4.14 EDS analysis of needle-shape crystal found in the microstructure

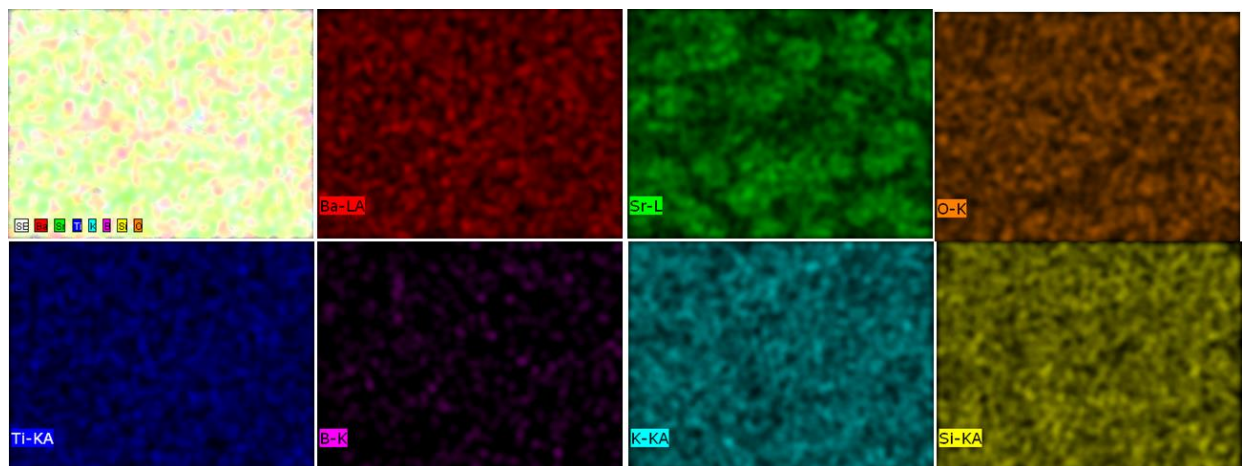


Figure 4.15 Elemental X-ray mapping showing the distributiun of elements from SBT base glass ceramic

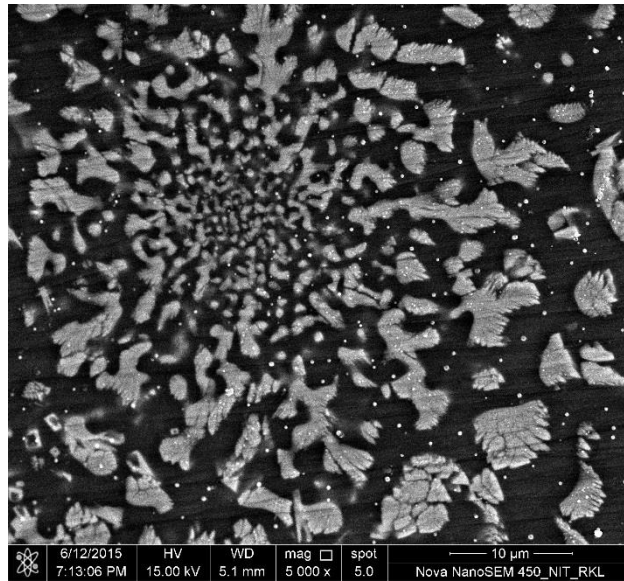


Figure 4.16 SEM image of 0.1 mol % La_2O_3 doped glass

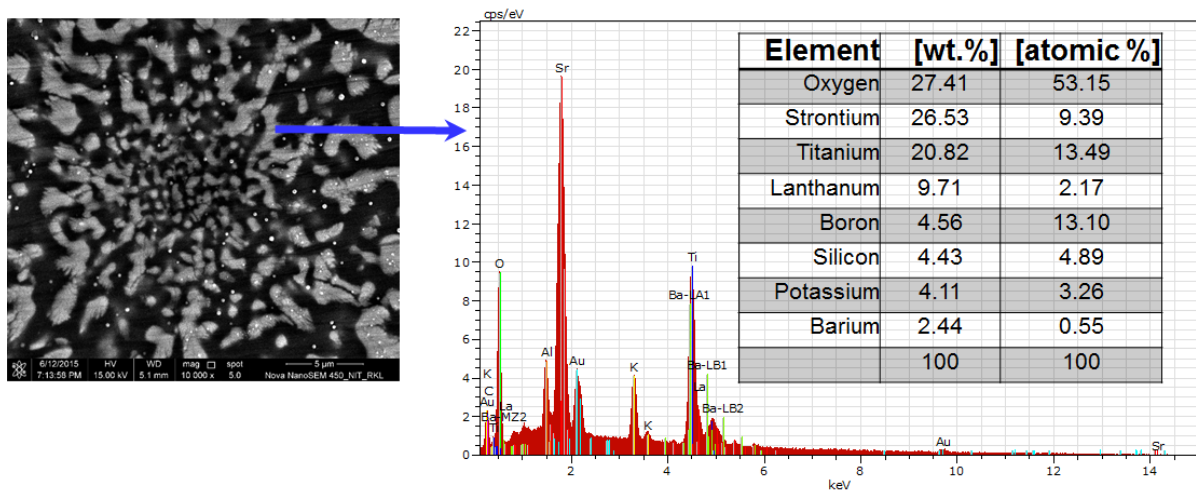


Figure 4.17 EDS analysis on the blocky irregular shaped interconnected crystals observed in the 0.1 mol % La_2O_3 doped glass ceramic sample

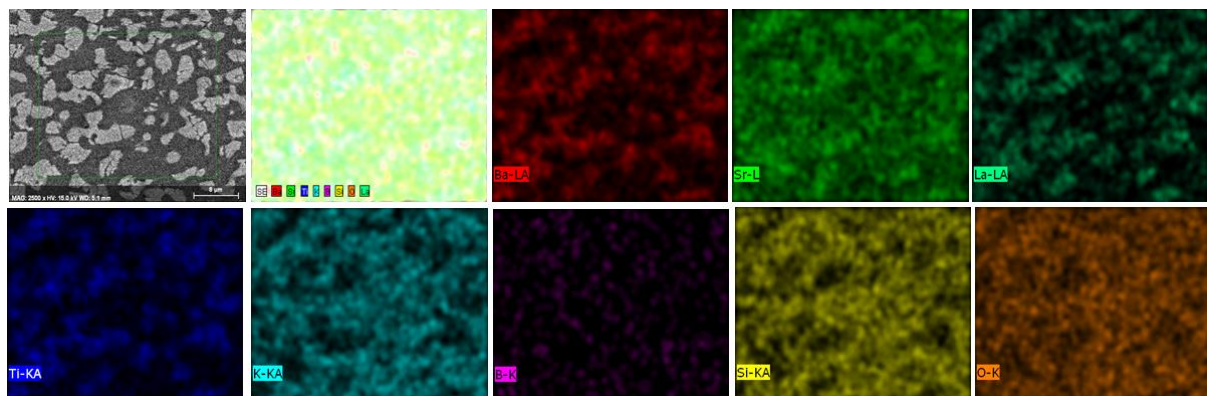


Figure 4.18 Elemental X-ray mapping showing the distributioun of elements from 0.1 mol % doped SBT glass ceramic

DIELECTRIC ANALYSIS

The dielectric properties of glass ceramics are controlled by factors such as the nature and amount of crystalline phases, crystallite size and morphology. The secondary phases, crystal clamping and the connectivity of the high permittivity perovskite crystals in the low permittivity glassy matrix. The nature of crystalline phases and micro-structure of glass ceramics can be controlled in the heat treatment conditions. The dielectric measurement at room temperature with varying frequency is also analysed.

From the **Figure 4.19** the dielectric result of the strontium barium titanate (SBT) base glass ceramics with varying frequency at room temperature can be observed. From the figure we could very well observe that the dielectric constant (ϵ) measured at room temperature remains constant (~ 18) with the measured frequencies 100Hz, 1 kHz, 10 kHz, 1000 kHz and 1 MHz. From the same figure we could also very well know the dielectric loss or dissipation factor ($\tan \delta$ or D). Here in this SBT base glass ceramics the loss factor is low i.e. < 0.1 . From the **Figure 4.20** the dielectric result of 0.1mol % La_2O_3 doped barium strontium titanate glass ceramics is observed. The 0.1mol % La_2O_3 doped SBT glass here gives the same result as SBT base glass ceramics i.e. ~ 30 with the same above measured frequencies i.e. 100Hz, 1 kHz, 10 kHz, 1000 kHz and 1 MHz at room temperature. However when the dielectric loss or dissipation factor ($\tan \delta$ or D) is considered some difference could be observed here in the case of 0.1mol % La_2O_3 doped SBT glass the loss is slightly more than the SBT base glass ceramics at room temperature i.e. < 0.08 .

From **Figure 4.21** the dielectric constant as well as the dissipation factor can be observed of SBT base glass ceramics. From the figure we could very well conclude that the dielectric constant gradually increases with increasing temperature at all frequencies however a distinctable changes of the value of dielectric constant could be observed in the **Figure 4.21** at low frequencies i.e. 100 Hz and 1 kHz. After 400 K it could be very well observed that the

dielectric constant values at low frequencies increases. The dielectric loss or dissipation factor also from the figure we could very well conclude that it gradually increases with increasing temperature at all frequencies however a distinctable changes of the value of dielectric loss or dissipation factor could be observed in the **Figure 4.21** at low frequencies i.e.100 Hz and 1 kHz. After 400 K it could be very well observed that the dielectric loss or dissipation factor values at low frequencies increases. However up to 400K there is a very low dielectric loss i.e. (0.001-0.15). Dielectric loss after 400 K is increased due to the movement of alkali ions present in the residual glass.

From **Figure 4.22** the dielectric constant and dielectric loss or dissipation factor of 0.1mol % La_2O_3 doped barium strontium titanate glass ceramics can be observed at different frequencies with varying temperature. The dielectric constant values and dielectric loss or dissipation factor values at all frequencies increases. The dielectric constant values here shows much higher values compared to SBT base glass ceramics. After 400 K the dielectric constant as well as dissipation factor increases exponentially. However there is a very low dielectric loss i.e. (0.001-0.2) up to 400 K. dielectric loss after 400 K increased likely due to the movement of alkali ions present in the residual glass.

A space charge polarization mechanism is likely responsible for the large observed dielectric constant of the BST glass ceramics doped with 0.1mol % La_2O_3 at low frequencies. La_2O_3 is considered to be A-site oxides in perovskite structures. La^{3+} has higher valences than (Ba^{2+} , Sr^{2+}).

Therefore, La_2O_3 additive can be viewed as donor dopant where it enters the BST lattice of glass ceramics, and thereby maintained the electrical charge neutrality according to the following possible Kröger–Vink notation. $3\text{Sr}^{2+} \rightarrow 2\text{La}^{3+} + V_{\text{Sr}}^\bullet$ $3\text{Ba}^{2+} \rightarrow 2\text{La}^{3+} + V_{\text{Ba}}^\bullet$
 $4\text{Sr}^{2+} + \text{Ti}^{4+} \rightarrow 4\text{La}^{3+} + V_{\text{Ti}}^\bullet$ $4\text{Ba}^{2+} + \text{Ti}^{4+} \rightarrow 4\text{La}^{3+} + V_{\text{Ti}}^\bullet$ $\text{Sr}^{2+} \rightarrow \text{La}^{3+} + e^-$
 $\text{Ba}^{2+} \rightarrow \text{La}^{3+} + e^-$ Electronic compensation should cause a substantial increase in conductivity,

in which the number of electron carriers equals the La^{3+} concentration. Free electron may accumulates at the BST/glass interface as space charge and increase the permittivity at low frequencies.

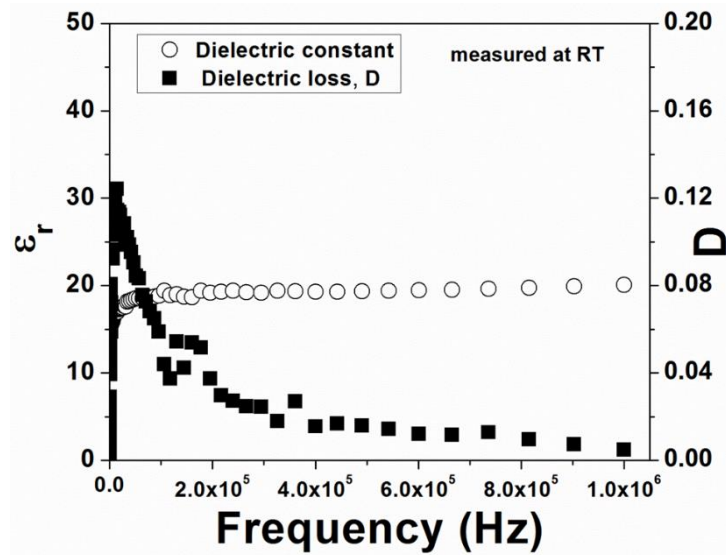


Figure 4.19 Dielectric measurement of SBT base glass ceramics at room temperature

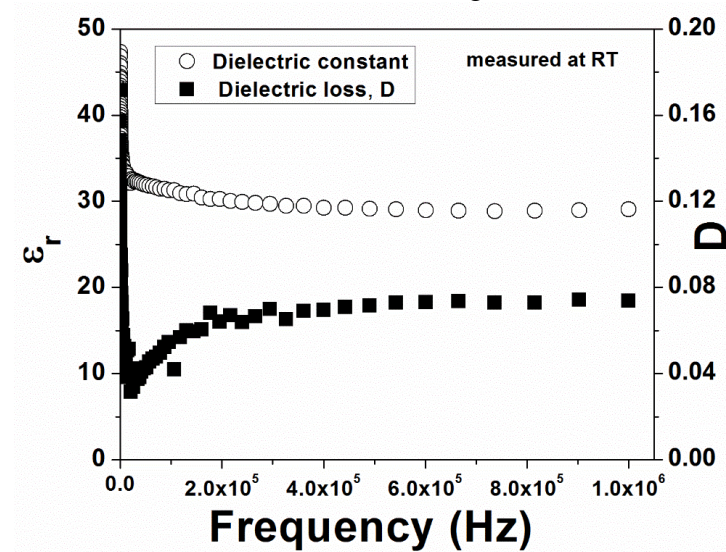
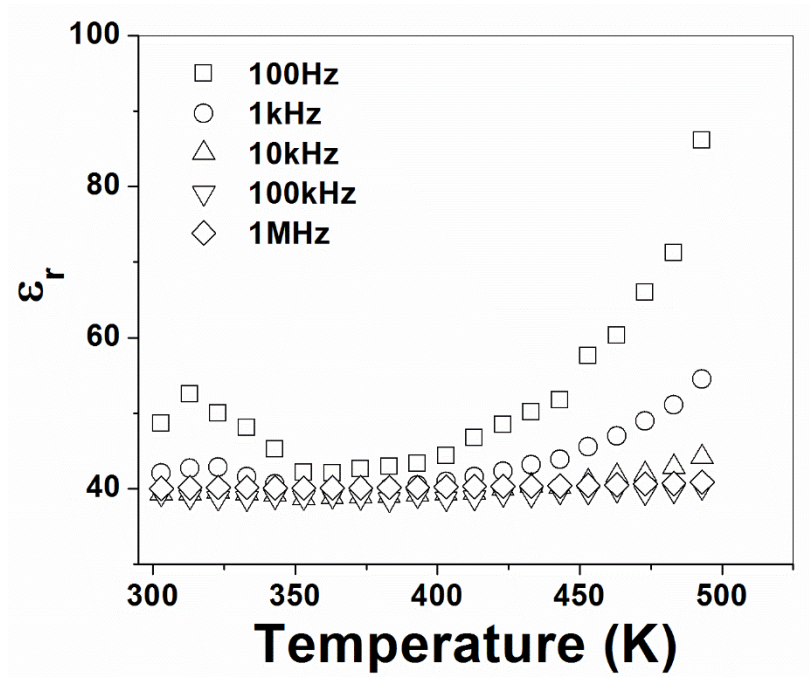
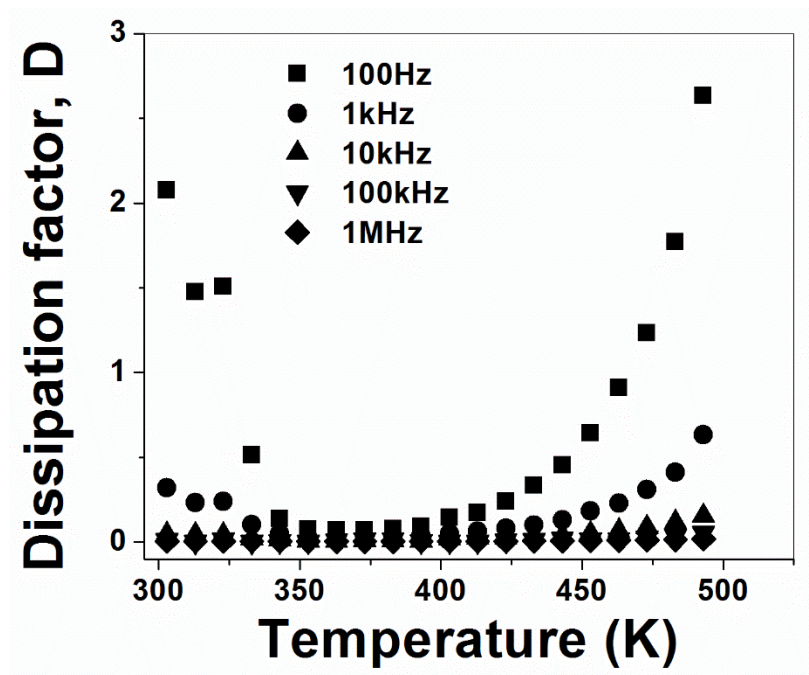


Figure 4.20 Dielectric measurement of doped glass ceramics at room temperature

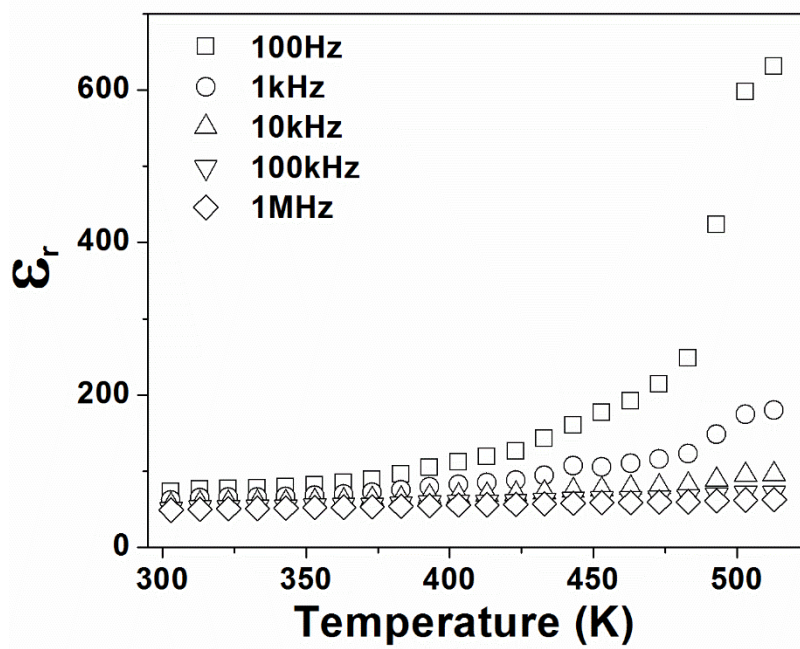


(a)

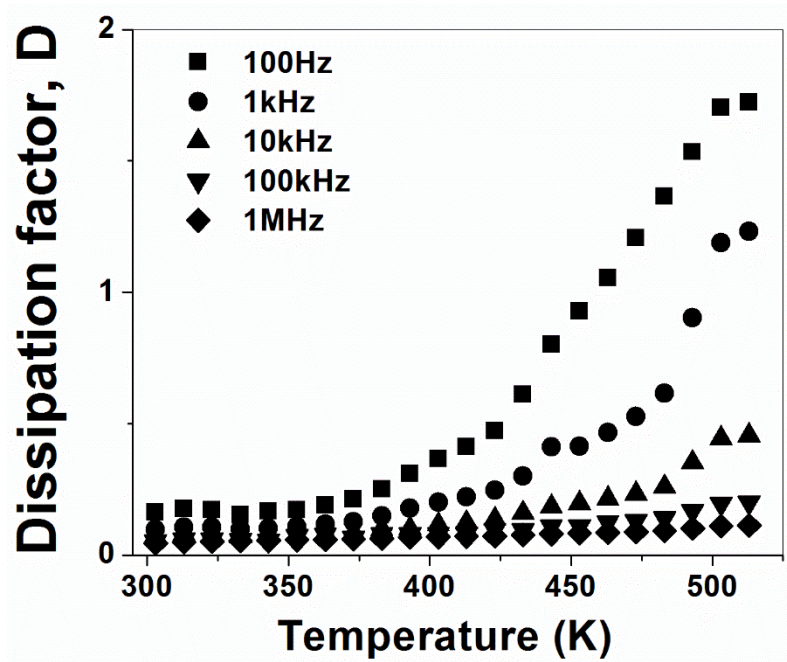


(b)

Figure 4.21 (a) Dielectric constant and (b) loss of SBT base glass ceramics with temperature



(a)



(b)

Figure 4.22 (a) Dielectric constant and (b) loss of 0.1mol % La_2O_3 doped SBT base glass ceramics with temperature

CONCLUSION

- SBT glass was successfully synthesized using melt-quench method.
- FTIR spectra of base glass and 0.1 mol% La_2O_3 doped glass shows the presence of stretching vibration of O–H bond inside the glassy network. Asymmetric stretching relaxation of the B–O bond of trigonal BO_3 units, stretching vibrations of B–O–Si linkage and deformation vibrations of the Si–O–Si bridges were also observed.
- DSC scan of base glass and doped glass reveals that addition of 0.1 mol% La_2O_3 addition into SBT base glass composition elevates the onset of crystallization temperature.
- XRD shows the formation of $\text{Sr}_2\text{TiSi}_2\text{O}_8$ and SiO_2 phase upon crystallization at 780°C for 3h in air for base glass sample obtained by air quench at room temperature. However, base glass sample obtained by melt-quench on a preheated graphite plate shows the formation of $\text{Sr}_{0.744}\text{Ba}_{0.2056}\text{TiO}_3$, SiO_2 and Ba_3SiO_5 phase. 0.1 mol% La_2O_3 doped glass sample upon crystallization at 750°C for 3h shows the formation of $\text{Sr}_{0.9}\text{La}_{0.1}\text{TiO}_3$, SiO_2 and Ba_3SiO_5 phase.
- SEM shows the formation of micron sized flower-like and needle shaped crystals precipitated throughout the microstructure in case of base glass ceramic sample. Addition of 0.1 mol % La_2O_3 modify the crystal structure to blocky precipitates.
- A space charge polarization mechanism is likely responsible for the large observed dielectric constant of the BST glass ceramics doped with 0.1mol % La_2O_3 at low frequencies. Free electron may accumulated at the BST/glass interface as space charge and increase the permittivity at low frequencies.

REFERENCE

- [1] Edgar Dutra Zanotto "A bright future for glass-ceramics", American Ceramic Society Bulletin, Vol. 89, No. 8.
- [2] Jiangying, W., Xi Yao, Liangying Zhang "Preparation and dielectric properties of barium strontium titanate glass-ceramics sintered from sol-gel-derived powders", *Ceramics International* 30 (2004) 1749–1752.
- [3] Gene H. Haertling (Ferroelectric Ceramics: History and Technology) *Journal of the American Ceramic Society—Haertling*.
- [4-5] A.S. Bhalla, R. Guo and R. Roy, (The perovskite structure – a review of its role in ceramic science and technology), *Mat. Res. Innovat.* 4, 3-26 (2000) and references there in.
- [6] Mats Johnsson and Peter Lemmens, (Crystallography and Chemistry of Perovskites),
- [7] A.F. Wells, (1995) *Structural Inorganic Chemistry*, Oxford Science publications U. Müller, (1993). *Inorganic Structural Chemistry*, Wiley & Sons Ltd
- [8-9] Xiangrong Wang, Yong Zhang *, Ivan Baturin , Tongxiang Liang (Blocking effect of crystal-glass interface in lanthanum doped barium strontium titanate glass ceramics), *Materials Research Bulletin* 48 (2013) 3817–3821.
- [10] Yong Zhang, Tao Ma, Xiangrong Wang, Zongbao Yuan and Qian Zhang, (Two dielectric relaxation mechanisms observed in lanthanum doped barium strontium titanate glass ceramics) *journal of applied physics* 28 April 2011.
- [11] Ozawa, T. *Bull. Chem. Soc. Jpn.*, 1965, 35, 1881.
- [12] P. G. Bray, "Interaction of Radiation with Solids," Plenum, New York, 1967.
- [13] R. V. Adams and R. W. Douglas, "Infrared Studies on Various Samples of Fused Silica with Special Reference to the Bands Due to Water," *Journal of the Society of Glass Technology*, Vol. 43, 1959, pp. 147-158.
- [14] H. Dunker and R. H. Doremus, "Short Time Reactions of a Na₂O-CaO-SiO₂ Glass With Water and Salt Solutions," *Journal of Non-Crystalline Solids*, Vol. 92, No. 1, 1987, pp. 61-72. doi:10.1016/S0022-3093(87)80359-9
- [15] R. D. Husung and R. H. Doremus, "Infrared Transmission Spectra of Four Silicate Glasses before and after Exposure to Water," *Journal of Materials Research*, Vol. 5, No. 10, 1990, pp. 2209-2217. doi:10.1557/JMR.1990.2209
- [16] G. Ramadevudu, S. R. L. Srinivasa, M. S. A. Hameed and M. C. Narasimha, "FTIR and Some Physical Properties of Alkaline Earth Borate Glasses Containing Heavy Metal Oxides," *International Journal of Engineering Science and Technology*, Vol. 3, No. 9, 2011, pp. 6998-7005.
- [17] N. A. Ghoneim, H. A. El Batal, N. Abdel Shafi and M. H. Azooz, "Synthesis and Characterization of Cadmium Doped Lead-Borate Glasses," *Proceeding of the Egyptian Conference of Chemistry*, Cairo, 1996, p. 162.

- [18] F. M. Ezz Eldin, N. A. E. L. Alaily, F. A. Khalifa and H. A. E. L. Batal, "In Fundamental of Glass Science and Technology," 3rd E.S.G. Conference Germany: Verlag Der Deutschen Lastechnischen Gesellschaft, 1995.
- [19] A. S. Tenny and J. J. Wong, "Vibrational Spectra of Vapour Deposited Binary Borosilicate Glasses," Chemical Physics, Vol. 56, No. 11, 1972, pp. 5516-5523.
- [20] H. Doweidar, M. A. A. Zeid and G. M. El-Damrawy, "Effect of Gamma Radiation and Thermal Treatment on Some Physical Properties of ZnO-PbO-B₂O₃ Glasses," Journal of Physics D, Vol. 24, No. 12, 1991, pp. 2222- 2228. doi:10.1088/0022-3727/24/12/015
- [21] M. Pal and B. Roy, "Structural Characterization of Borate Glasses Containing Zinc and Manganese Oxides," Journal of Modern Physics, Vol. 2, No. 9, 2011, pp. 1062-1066. doi:10.4236/jmp.2011.29129
- [22] K. El-Egili, "Infrared Studies of Na₂O-B₂O₃-SiO₂ and Al₂O₃-Na₂O-B₂O₃-SiO₂ Glasses," Physic B, Vol. 325, 2003, pp. 340-348. Doi: 10.1016/S0921-4526(02)01547-8
- [23] A.K. Yadav, C.R. Gautam, P. Singh, New J. Glass Glass Ceram. **2**, 126 (2012)